

In Vitro Evaluation of a Targeted and Sustained Release System for Retinoblastoma Cells Using Doxorubicin as a Model Drug

Sai H.S. Boddu, Jwala Jwala, Monica R. Chowdhury, and Ashim K. Mitra

Abstract

Purpose: The objective of this study was to develop a novel folate receptor-targeted drug delivery system for retinoblastoma cells using doxorubicin (DOX) as a model drug.

Methods: Biodegradable DOX-loaded poly(D,L-lactide-co-glycolide)-poly(ethylene glycol)-folate (PLGA-PEG-FOL) micelles (DOXM) were prepared with various solvents (dimethylsulfoxide, acetone, and dimethylformamide). The effects of solvents on entrapment efficiency, particle size, and polydispersity were examined. The effects of thermosensitive gel structure on the release of DOX from the DOXM were also studied. Qualitative and quantitative uptake studies of DOX and DOXM were carried out in Y-79 cell line. Cytotoxicity studies of DOXM were performed on Y-79 cells.

Results: Based on size, polydispersity, and entrapment efficiency, dimethylformamide was found to be the most suitable solvent for the preparation of DOXM. Dispersion of DOXM in PLGA-PEG-PLGA gel sustained drug release for a period of 2 weeks. Uptake of DOX was ~4 times higher with DOXM than DOX in Y-79 cells overexpressing folate receptors. This was further confirmed from the quantitative uptake studies. DOXM exhibited higher cytotoxicity in Y-79 cells when compared with pure DOX.

Conclusion: These polymeric micellar systems suspended in thermosensitive gels may provide sustained and targeted delivery of anticancer agents to retinoblastoma cells following intravitreal administration.

Introduction

RETINOBLASTOMA (RB) REPRESENTS A common form of intraocular malignancy affecting the retina.^{1,2} Eighty-seven percent of children who are diagnosed with RB do not survive very long because of invasion, metastasis, and hematogenous spread.^{3,4} It is common in children between the age of 3 and 7.⁵ Reese-Ellsworth (RE) classification system is applied most widely for describing intraocular tumors.^{6,7} As per the classification, RB tumor is divided into 5 groups as shown in Table 1. Although it is not a real staging system it has served as an excellent tool for determining and comparing different treatment strategies. RE groups IV and V are considered as very advanced and do not respond well to chemotherapy.⁸ In such cases, external beam radiotherapy (EBR) and enucleation are employed as the last recourse. Both treatments leave the survivors with complete or nearly complete vision loss.⁹ Currently, EBR is no longer a viable option because of long-term side effects such as optic neuropathy, cataract, retinopathy, and chronic dry eye.¹⁰ Development of secondary tumors in the area exposed to radiation after a long

time period is the major reason that discourages the application of EBR.¹⁰ Enucleation is the only treatment option for RE group V tumors.

In the last decade, several reports suggest that chemotherapy is successful in treating the RE groups I to III tumors.⁸ This is due to the presence of vitreal seeds that are responsible for disease recurrence.⁹ However, exposing the eye to another external beam radiation may result in complications caused by a high radiation dose. Chemotherapy helps in the reduction of vitreal seeds and tumor size, so that focal therapy (photocoagulation, hyperthermia, cryotherapy, or radioactive plaque) can be applied to a relatively small area and tumor can be shrunk without loss of vision.^{8,11,12} Systemic chemotherapy for RB was introduced in the 1960s. Recent work has explored the use of topotecan, etoposide, carboplatin, and vincristine for the treatment of RB.^{8,13} Some investigators have added cyclosporine in the regimen as a P-glycoprotein (P-gp) inhibitor assuming that anticancer agents will show better efficacy, but this therapeutic regime remains controversial.¹⁴ One of the major impediments to drug development in RB has been the lack of knowledge

TABLE 1. REESE-ELLSWORTH SYSTEM FOR INTRAOCULAR RETINOBLASTOMA

Group I Very favorable	Solitary tumor, <4 disc diameters in size, at or behind the equator Multiple tumors, none >4 disc diameters in size, all at or behind the equator
Group II Favorable	Solitary tumor, 4–10 disc diameters in size, at or behind the equator Multiple tumors, 4–10 disc diameters in size, behind the equator
Group III Doubtful	Any lesion anterior to the equator Solitary tumors >10 disc diameters behind the equator
Group IV Unfavorable	Multiple tumors, some >10 disc diameters Any lesion extending anteriorly to the ora seratta
Group V Very unfavorable	Massive tumors involving over half the retina Vitreous seeding

regarding intraocular disposition, elimination, blood ocular transport, and retinal uptake of chemotherapeutic agents. For effective therapy, chemotherapeutic agents should enter tumor cells in required therapeutic concentrations. Generally, chemotherapeutic agents are administered by intravenous route, which, in the absence of any targeting strategy, exposes normal cells to high levels of anticancer agents, resulting in cytotoxicity.¹³ In addition, initial drug exposure causes upregulation of multidrug-resistant (MDR) genes, resulting in increased expression of efflux pumps (P-glycoprotein (P-gp), multidrug resistance protein (MRP), and breast cancer resistance protein (BCRP) leading to increased drug efflux.¹⁵ RB cells are known to express efflux proteins such as P-gp and MRP.^{16,17} Most of the chemotherapeutic agents are good substrates for these efflux pumps, which reduces drug concentrations in retinal tissues.^{18,19}

In the past few years, research in drug delivery to the posterior segment by intravitreal (IVT) injections has grown significantly. Although IVT injections can achieve therapeutic drug concentrations in the neural retina, adverse effects such as retinal detachment from repeated injections, hemorrhage, endophthalmitis, and other retinal toxicities due to high drug concentrations achieved from IVT bolus dose administration may result in patient noncompliance.²⁰ Direct IVT administration of chemotherapeutic agents lead to drug-induced cataract in the lens and clouding of the cornea.²¹ An ideal drug delivery system for the treatment of RB should possess high encapsulation efficiency and should selectively deliver drugs to tumor cells in a sustained manner.

Drug targeting via receptors is an effective way to cell-selective drug delivery, because this process allows a satisfactory transport rate and ligand-dependent cell specificity. Folic acid, an essential vitamin, enters into cells through a membrane-associated folate-binding protein in addition to a classical high-affinity/low-capacity carrier system.^{22,23} Targetability of various delivery systems such as liposomes, polymer conjugates, polymeric micelles, and nanoparticles has been achieved with a covalently attached folate on the surface.²⁴ For chemotherapeutics agents such as doxorubicin (DOX), biodegradable polymeric micelles have been utilized for passive and active targeting to various solid tumors.^{24,25} Selective targeting and higher cytotoxicity in folate receptor-positive cancer cells have been achieved with folate-conjugated polymeric micelles.^{24,26} However, no studies have been reported regarding the effectiveness of polymeric micelles in the treatment of intraocular tumors. Drugs entrapped inside polymeric micelles are released rapidly within a short span of 24–48 h. Yoo and Park conjugated DOX to poly(D,L-lactide-co-glycolide)-poly(ethylene glycol) (PLGA-PEG) block copolymer and utilized this construct for the

preparation of polymeric micelles. DOX-PLGA-PEG micelles exhibited sustained drug release for 2–3 weeks.²⁷ However, this strategy is tedious and expensive because the chemistry involved in the conjugation of a polymer to a ligand needs to be optimized for each drug.

In this study, we made an attempt to develop and evaluate a novel folate receptor-targeted drug delivery system for RB cells. DOX, a fluorescent molecule, was used as a model drug for the studies. Previous studies from our laboratory have confirmed the presence of folate receptors on RB (Y-79) cell line.²⁸ We have synthesized PLGA-PEG-folate (FOL) for selective delivery to RB cells. Biodegradable DOX-loaded PLGA-PEG-FOL micelles (DOXM) were prepared from various solvents [dimethylsulfoxide (DMSO), acetone, and dimethylformamide (DMF)]. The effects of solvents on entrapment efficiency, size, and polydispersity were examined. Further, the effects of thermosensitive gel (PLGA-PEG-PLGA) on the release of DOX from DOXM were also described.

Methods

Materials

Polyoxyethylene bis(amine) (M_w 3,000), folic acid, DOX HCl, DMSO, dicyclohexylcarbodiimide (DCC), triethylamine (TEA), acetone, PEG 1450, and dialysis tubing made of cellulose membrane were procured from Sigma Chemicals. Resazurin dye was obtained from Biotium. DMF was obtained from American Scientific Products. PLGA (RG502H) [weight average molecular weight (M_{wb}): 8,000] was obtained from Boehringer Ingelheim. The thermosensitive gel PLGA-PEG-PLGA (M_{wb} : 4,759 Da) was synthesized and purified.

Synthesis of PLGA-PEG-FOL

PLGA-PEG-FOL was synthesized according to a previously published procedure with minor modifications: step I—activation of PLGA; step II—synthesis of PLGA-PEG-NH₂; step III—synthesis of PLGA-PEG-FOL.²⁴

Step I—activation of PLGA. PLGA was activated with DCC and *N*-hydroxysuccinimide (NHS) in dichloromethane (molar ratio of DCC:NHS:PLGA = 1.2:1.2:1) under inert atmosphere for 24 h. Activated PLGA was precipitated with ice-cold diethyl ether followed by filtration and vacuum drying for 24 h.

Step II—synthesis of PLGA-PEG-NH₂. One gram of activated PLGA was dissolved in dichloromethane (5 mL). In a separate flask, 2.1 g of PEG-bis-amine was dissolved in 2 mL of dichloromethane and added to PLGA solution in a

dropwise manner (PLGA:PEG-bis-amine = 1:5). The reaction mixture was stirred under inert atmosphere. PLGA-PEG-NH₂ was dialyzed (Molecular weight cut-off [MWCO]: 10 kDa) against deionized water for 48 h to remove unreacted PEG-bis-amine and freeze dried (VirTis Wizard 2.0 Freeze Dryer Control System).

Step III—synthesis of PLGA-PEG-FOL. Folic acid was activated with NHS and DCC at a molar ratio of folic acid/NHS/DCC = 1:2:2. Folate-conjugated di-block copolymer was synthesized by coupling PLGA-PEG-NH₂ (500 mg) in DMSO to activated folic acid. The reaction was performed under inert atmosphere at room temperature for 12 h. The reaction mixture was mixed with 50 mL of distilled water and centrifuged at 5,000 g and the pellet of dicyclohexa was discarded. The supernatant was dialyzed (MWCO: 10 kDa) extensively against deionized water for 48 h and then freeze dried.

Characterization of PLGA-PEG-FOL

The structure of PLGA-PEG-FOL was confirmed by ¹H NMR spectroscopy (Varian-400 MHz NMR spectrometer) in *d*₆-DMSO. Chemical shifts (δ) were expressed in parts per million (ppm) relative to the NMR solvent signal (*d*₆-DMSO) using tetramethyl silane as an internal standard. Amount of folic acid conjugated to PLGA-PEG-FOL was determined by a calibration curve of folic acid generated in DMSO at 340 nm.

Preparation of DOXM

DOX was neutralized with 2 mol excess of TEA in 2 mL of DMSO, acetone, or DMF. Dialysis tubing used in the study was resistant to DMSO, acetone, or DMF. Briefly, 5 mg of DOX (after TEA treatment) and 20 mg of PLGA-PEG-FOL were dissolved in 5 mL of DMSO, acetone, or DMF and vortexed for 10 min. This solution was dialyzed (MWCO: 10 kDa) for a period of 48 h against distilled deionized water to remove solvent and untrapped DOX. Micelles thus formed were freeze dried and characterized for entrapment efficiency, particle size, polydispersity, morphology, and *in vitro* release characteristics.²⁵ PLGA-PEG micelles of DOX (DOXMC) were also prepared in a similar manner and used as control in the uptake studies.

Entrapment efficiency studies

Two milligrams of freeze-dried DOXM was dissolved in DMSO and DOX content was analyzed using a microplate reader (DTX 880 Series Multimode Detector, Multimode Detection Software; Beckman Coulter) at 485 nm (excitation wavelength) and 595 nm (emission wavelength). Entrapment efficiency was calculated using equation (1). All experiments were conducted in triplicates.

$$\text{Entrapment efficiency (\%)} = \frac{\text{Weight of drug in micelles}}{\text{Weight of drug fed initially}} \times 100 \quad (1)$$

Particle size analysis

Dynamic light scattering (Brookhaven Zeta Plus instrument) technique was employed to measure the particle size of DOXM. Polydispersity values were also measured.

Morphology of polymeric micelles

Transmission electron microscopy (TEM; Philips CM12 STEM) was utilized to examine the morphology of polymeric micelles. A drop of micellar solution was placed on a carbon-coated copper grid and excess of fluid was removed by a piece of filter paper. The sample was then stained with 2% phosphotungstic acid solution and excess solution was removed using a filter paper. TEM images were taken after the sample was completely dried.

In vitro drug release

Five milligrams of DOXM was dispersed in 1 mL isotonic phosphate buffer saline (pH 7.4) or 1 mL of 23% (w/v) PLGA-PEG-PLGA polymer solution and subsequently introduced into dialysis bags (MWCO: 6,275 g/mol). The polymer solution inside the bags was allowed to form a gel at 37°C for 30–60 s. The dialysis bags were introduced into vials containing 10 mL isotonic phosphate buffer saline and 0.025% (w/v) sodium azide to avoid microbial growth and 0.02% (w/v) Tween-80 to maintain sink condition. The vials were placed in a shaker bath with temperature maintained at 37°C ± 0.5°C and constant agitation of 60 oscillations/min. At regular time intervals, 200 μL samples were withdrawn and replaced with equal volumes of fresh buffer. Samples were analyzed with a microplate reader at 485 nm (excitation wavelength) and 595 nm (emission wavelength). All experiments were conducted in triplicates.

Morphology of polymeric micelles suspended in thermosensitive gels

Scanning electron microscopy (FEG ESEM XL 30; FEI) was employed for studying surface morphology. The thermosensitive gels with suspended freeze-dried powder of polymeric micelles were attached to a double-sided tape, spray-coated with gold-palladium at 0.6 kV, and then examined under a electron microscope.

Cell culture

Human RB cell line (Y-79) was obtained from American Type Culture Collections. Y-79 cells were used for estimating the qualitative and quantitative uptake of DOX from micelles. Further cytotoxicity studies were also performed on these cells. Y-79 cells were incubated in 75-cm² tissue culture flasks as a suspension in RPMI-1640 medium supplemented with 15% nonheat-inactivated fetal bovine serum, 1 mM glutamine, penicillin (100 U/mL), and streptomycin (100 μg/mL). The cells were maintained at 37°C in a humidified atmosphere of 5% CO₂ and 90% relative humidity.

Uptake studies

Y-79 cells were centrifuged and washed 3 times with a Dulbecco's phosphate-buffered saline (DPBS; pH 7.4) containing 0.03 mM KCl, 130 mM NaCl, 1 mM CaCl₂, 7.5 mM Na₂HPO₄, 1.5 mM KH₂PO₄, 0.5 mM MgSO₄, and 5 mM glucose to remove endogenous folates bound to folate receptors on the cell surface. Uptake studies were carried out in DPBS (pH 7.4). Uptake was initiated by the addition of 200 μg/mL of DOX solution, DOXMC, DOXM, and DOXM solution in the presence of excess folic acid (~1 mM) for 1 h. After incubation, the cells were centrifuged and rinsed 3 times with

1 mL of ice-cold stop solution (210 mM KCl, 2 mM HEPES) to arrest uptake. After each wash, the cells were centrifuged and separated. The cells were then solubilized in 0.5 mL of 1% Triton-X solution and frozen at -80°C . DOX concentration was measured with the help of fluorescence spectrophotometer at 485 nm (excitation wavelength) and 595 nm (emission wavelength).²⁸

Confocal studies

Y-79 cells were incubated with DOX solution, DOXM, and DOXM in the presence of excess folic acid (~ 1 mM) for 30 min in DPBS. DOX concentration equivalent to $10\ \mu\text{g}/\text{mL}$ was maintained in the solutions. Following incubation the cells were washed 3 times to remove uninternalized DOX, then exposed to 4% buffered paraformaldehyde for 20 min at 4°C , rinsed thrice with DPBS, and mounted on glass slides using mounting gel. Slides were observed under a confocal laser fluorescence microscope. Series of images were acquired in the z-axis ($0.5\ \mu\text{m}$ apart) with Olympus FV300 confocal laser scanning unit coupled to an Olympus BX61 upright microscope. Pictures were processed by Fluoview™ software and edited by Adobe Photoshop CS3 (Adobe Systems).

Cell viability studies in Y-79 cells

As Y-79 cells do not attach to the substratum, the 96-well plates were initially coated with coated $50\ \mu\text{g}/\text{mL}$ poly-D-lysine solution. Approximately, 5,000 cells/well were plated and incubated with RPMI-1640 medium containing laminin

($12.5\ \mu\text{g}/\text{mL}$, added to the medium) at 37°C for 24 h. The cells were then exposed to various concentrations (0 – $10\ \mu\text{M}$) of DOX solution and DOXM. The cells with medium alone were used as negative control. The cells were incubated for 48 h, drug solutions were aspirated, and then $100\ \mu\text{L}$ of resazurin dye solution was added to each well. The plate was incubated for 1 h at 37°C and the amount of absorbance in each well was measured at 600 nm. Resazurin is a blue-colored compound that turns pink upon oxidation in the presence of live cells. The amount of absorbance reflects the number of viable cells.

Results

Biodegradable copolymer PLGA-PEG-FOL was successfully synthesized according to a previously published procedure with minor modifications.²⁴ Chemical shifts (δ) were expressed in ppm relative to the NMR solvent signal (d_6 -DMSO) with tetramethyl silane as an internal standard. Figure 1 demonstrates various proton peaks associated with PLGA-PEG-FOL polymer. Small peaks at 6.6, 7.6, and 8.7 ppm indicate protons associated with folate. The peak at 3.6 ppm is due to $-\text{CH}_2-$ protons of PEG block. The peaks at 1.6 and 5.2 ppm are due to $-\text{CH}_3$ and $-\text{CH}-$ protons of PLA block. The peak at 4.8 ppm belongs to the $-\text{CH}_2-$ protons of PGA block. On molar ratio basis the conjugation percentage of folate to PLGA-PEG was found to be 52.7%. DOXM were successfully prepared by dialysis method. Table 2 shows the effect of particle size, polydispersity, and entrapment of DOX in various solvents. Based on size, polydispersity, and

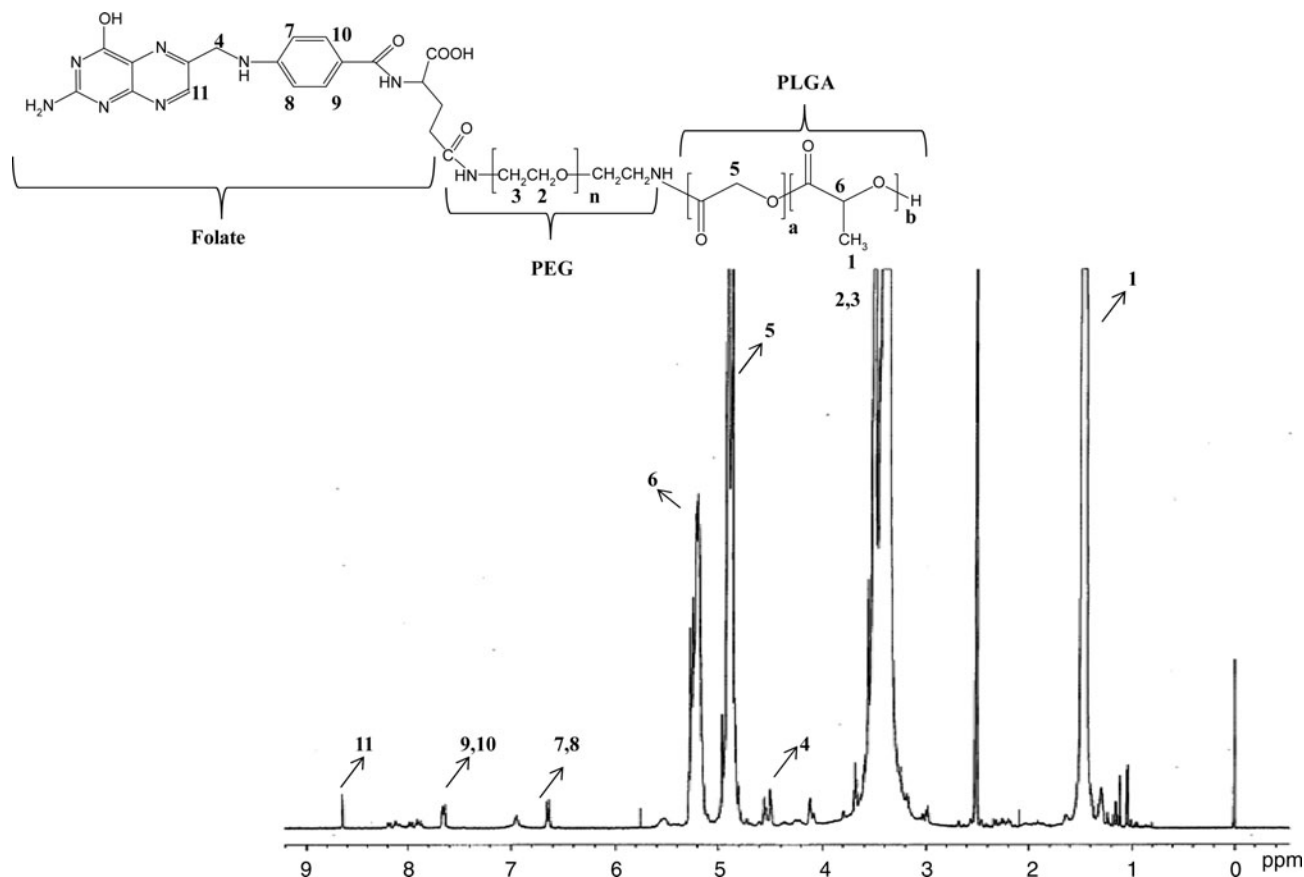


FIG. 1. ^1H NMR spectrum of poly(D,L-lactide-co-glycolide)-poly(ethylene glycol)-folate (PLGA-PEG-FOL) conjugate. The corresponding proton peak numbers marked in the NMR are denoted in the inset structure of PLGA-PEG-FOL.

TABLE 2. EFFECTS OF SOLVENTS ON PARTICLE SIZE, POLYDISPERSITY, AND ENCAPSULATION EFFICACY OF DOXORUBICIN

Solvent	Particle size (nm)	Polydispersity	Encapsulation efficiency (%)
DMSO	85.30 ± 4.53	0.31	58.20 ± 2.01
Acetone	101.20 ± 5.63	0.23	52.45 ± 3.74
DMF	75.20 ± 2.40	0.08	60.32 ± 2.56

Abbreviations: DMF, dimethylformamide; DMSO, dimethylsulfoxide.

entrapment efficiency, DMF was found to be suitable for the preparation of DOXM. The particle size of DOXM in DMSO, acetone, and DMF were observed to be 85.30, 101.20, and 75.20 nm, with a polydispersity of 0.31, 0.23, and 0.08, respectively. The entrapment efficiencies of DOX in DMSO, acetone, and DMF were found to be 58.20%, 52.45%, and 60.32%, respectively. DOXM were further characterized for morphology and *in vitro* release. The spherical morphology of DOXM was confirmed by TEM studies (Fig. 2). *In vitro* drug release study revealed a biphasic release pattern with an initial rapid release (burst release) followed by sustained release for a period of 48 h (Fig. 3). The release of DOX from DOXM was retarded in the presence of PLGA-PEG-PLGA gel. The synthesis and characterization of the triblock copolymer PLGA-PEG-PLGA (M_{wb} determined by gel permeation chromatography is 4,759 Da) has been already published from our laboratory.²⁹ Phase-transition studies revealed that the polymer at concentrations ranging between 20% and 25% (w/v) forms gel at 32°C–60°C.²⁹ As the temperature inside the eye ranges from 34°C to 37°C, such polymeric gels may be appropriate for drug delivery (Fig. 4A and B).³⁰ PLGA-PEG-PLGA gel sustained the release of DOX for a period of 132 h. Surprisingly, the dispersion of folate-conjugated polymer micelles in the PLGA-PEG-PLGA gel structure sustained the drug release for a period of 2 weeks (Fig. 3). Scanning electron microscopy image of DOXM dispersed in thermosensitive gels revealed a very dense network structure (Fig. 4C). The reversibility of the PLGA-PEG-PLGA gel was tested by slowly reducing the temperature from 37°C to 25°C, to achieve a clear solution (Fig. 4D). The uptake of DOX from pure drug solution, DOXM, and DOXM in the presence of folic acid was analyzed with confocal microscopy in Y-79 cells. DOXM exhibited higher fluorescence relative to free DOX (Fig. 5A and B). The fluorescence intensity was reduced in the presence of excess folic acid, suggesting uptake of micelles via folate receptor (Fig. 5C). Z-stack images were taken to confirm the presence of DOXM inside Y-79 cells (Fig. 5D–K). The uptake of both DOX and DOXM was quantitatively estimated in Y-79 cells. The uptake of DOX was ~4 times higher in the presence of DOXM (Fig. 6). Cytotoxicity studies of DOX formulations (free DOX and DOXM) were carried out in RB cell line (Y-79 cells). At concentrations ranging from 0 to 10 μM, DOXM exhibited higher cytotoxicity in Y-79 cells expressing folate receptors (Fig. 7).^{31,32}

Discussion

Systematically administered antineoplastic agents exhibit limited permeability into the retina and vitreous mainly

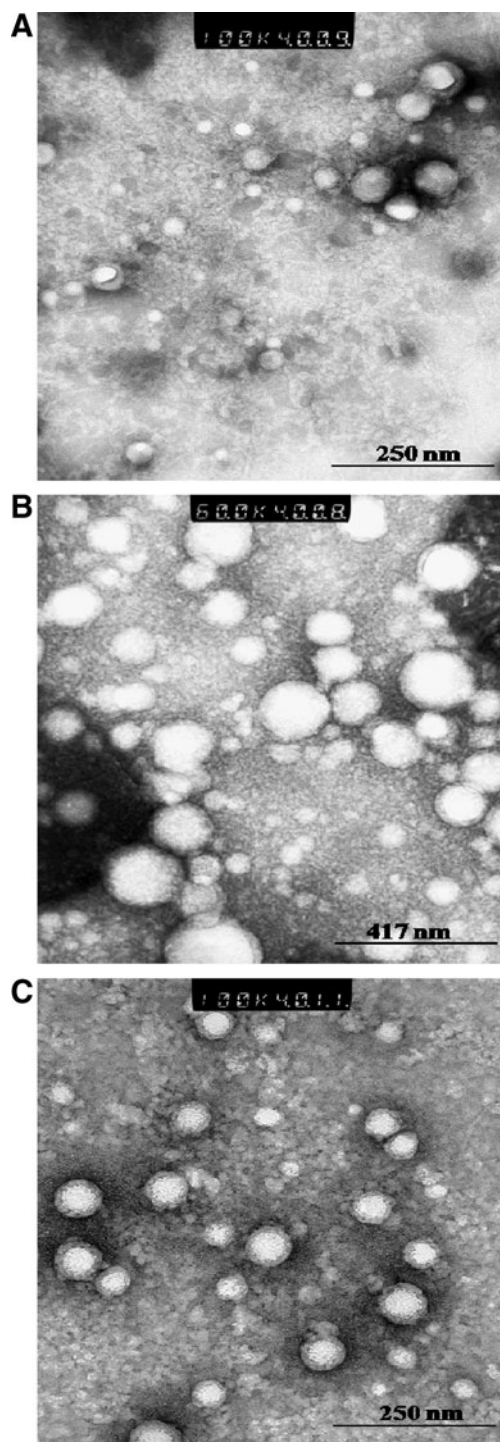
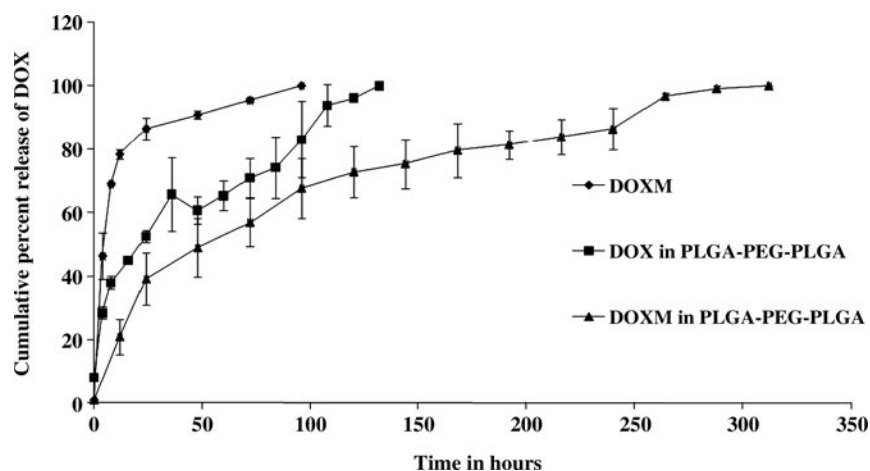


FIG. 2. Transmission electron microscopy image of doxorubicin-loaded PLGA-PEG-FOL micelles (DOXM). (A) DOXM prepared by dimethylsulfoxide; (B) DOXM prepared by acetone; (C) DOXM prepared by dimethylformamide.

because of blood retinal barrier.²⁰ Moreover, the presence of efflux pumps such as P-gp and MRP further restrict the permeation of various chemotherapeutic agents.³³ Although IVT injections deliver drugs to the retina directly, potential side effects such as increased intraocular pressure, hemorrhage, retinal detachment, cataract, and endophthalmitis lead to complications limiting long-term therapy.²⁰ Recent

FIG. 3. *In vitro* release profile of DOX from (◆) DOXM, (■) DOX suspended in PLGA-PEG-PLGA thermosensitive gel, and (▲) DOXM suspended in PLGA-PEG-PLGA thermosensitive gel. Each data point is the average of 3 samples. Error bars represent the standard error of mean.



advances in drug delivery system design led to the development of IVT implants that can be placed inside the vitreous to deliver constant drug levels over prolonged periods. However, such a system requires repeated surgery for the implantation and removal of implants.²⁰ Keeping these facts in mind we have developed an alternative strategy that employs *in situ* gelling polymers for sustaining drug release from surface-modified polymeric micelles targeting drugs to RB cells. Polymeric micelles have been successfully utilized as targeted drug delivery systems.³⁴ However, polymeric micelles tend to dissociate upon dilution in biological fluids after injection, which results in burst release.³⁵ The exact

mechanism involved in the destabilization of polymeric micelles is not clear. Recent studies by Chen *et al.* revealed that potential interactions of polymeric micelles with various biological components may affect the release pattern of entrapped drugs.³⁶ We hypothesized that thermogelling systems (PLGA-PEG-PLGA) as delivery vehicles might prevent the dilution and interaction of polymeric micelles with biological components.

Previous studies reported 44.8% (molar ratio basis) conjugation of folate to PLGA-PEG.²⁴ In the present study, the conjugation of folate was found to be 52.7%. At a fixed ratio of drug to polymer of 1:4, the effects of solvents on entrapment

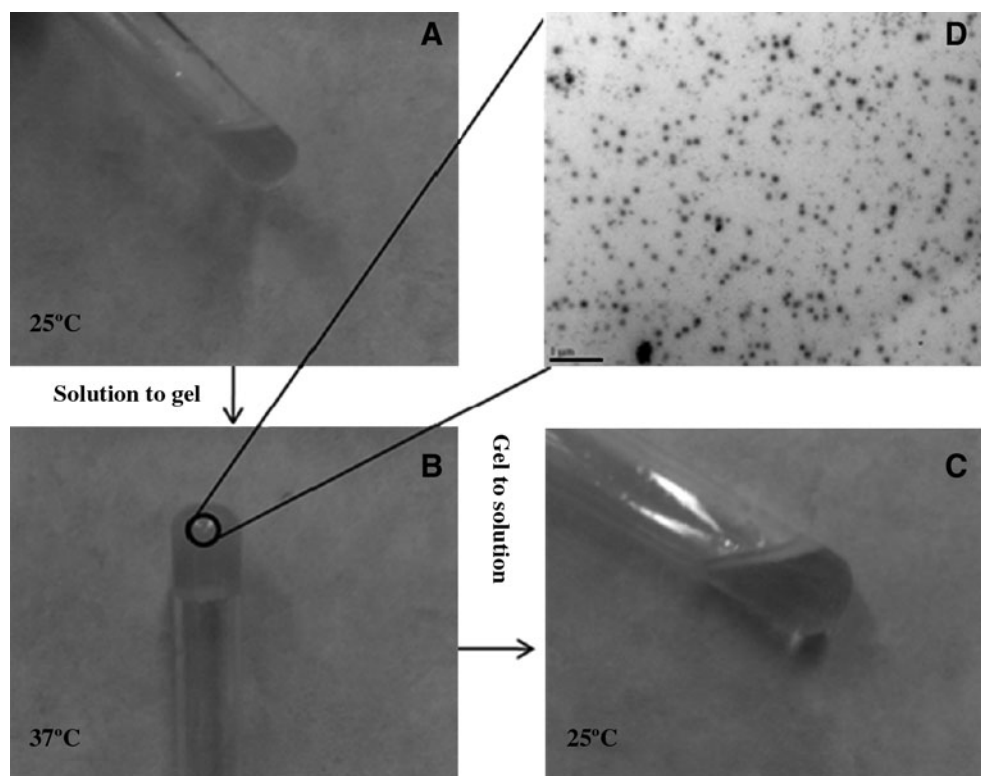


FIG. 4. Gelation and uniform dispersion of polymeric micelles in PLGA-PEG-PLGA thermosensitive gel. (A) DOXM suspended in PLGA-PEG-PLGA thermosensitive gel at 25°C; (B) DOXM suspended in PLGA-PEG-PLGA thermosensitive gel at 34°C–37°C; (C) scanning electron microscopy images of DOXM suspended in PLGA-PEG-PLGA thermosensitive gel; (D) reverse transition of gel to solution at 25°C.

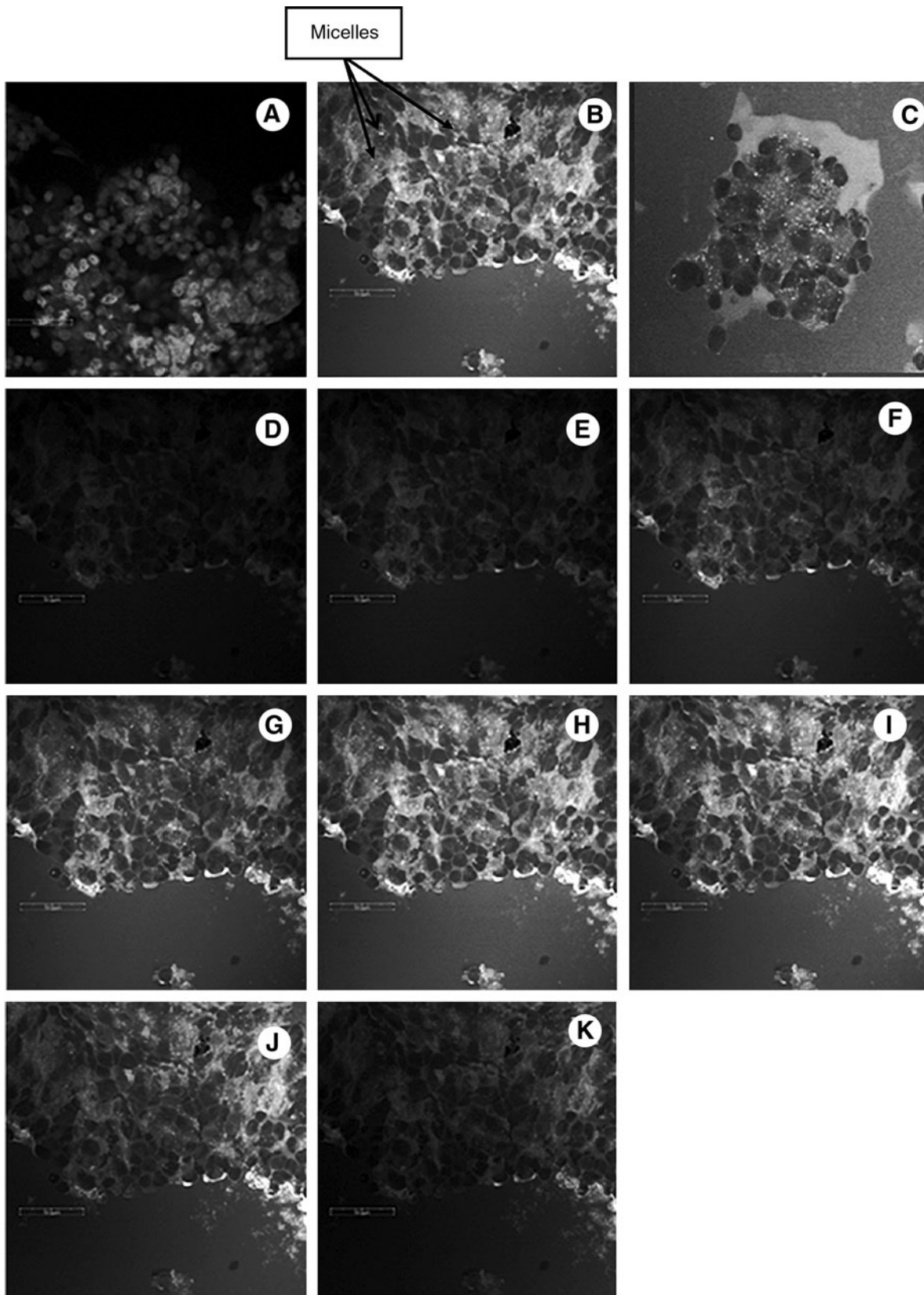


FIG. 5. Confocal images of Y-79 cells following treatment with DOX and DOXM. (A) Pure DOX; (B) DOXM; (C) DOXM in the presence of folic acid; (D–K) Z-stack images of DOXM to show that micelles are inside Y-79 cells. Scale bar = 50 μ m.

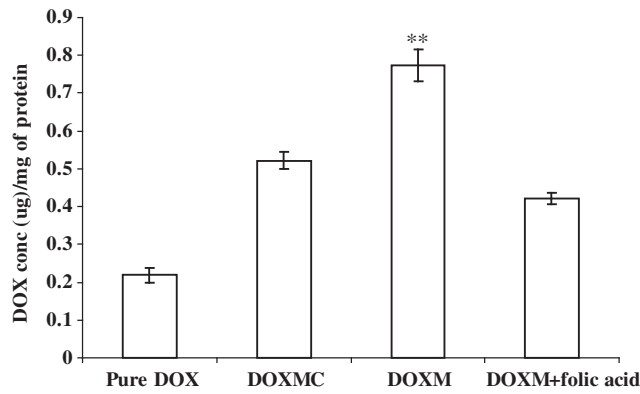


FIG. 6. Quantitative uptake of DOX in Y-79 cells, using pure DOX, DOX-loaded in PLGA-PEG micelles/nontargeted micelles (DOXMC), DOXM, and DOXM in the presence of folic acid. ** $P < 0.05$.

efficiency, size, and polydispersity were studied. DMF resulted in low polydispersity values, indicating uniform micellar size when compared with DMSO and acetone. The particle size of DOXM was found to be higher in case of acetone. Slight variations in entrapment efficiency and size may be attributed to the differences in miscibility/solubility of organic solvents in water.³⁷ Further characterization was carried out for DOXM prepared from DMF as the initial solvent. DOX release rate was faster from DOXM in the first 8 h and then became progressively lower and sustained for 48 h thereafter. The release from polymeric micelles mainly involves 2 mechanisms: diffusion and copolymer degradation. However, several studies suggest that when the rate of drug release is greater than the rate of copolymer degradation, diffusion mechanism predominates.³⁸ Burst release is mainly due to the DOX molecules adsorbed within the corona or at the interface of core/corona.²⁵ When dispersed in PLGA-PEG-PLGA thermosensitive gels, *in vitro* release of DOX from DOXM was sustained for 2 weeks. The exact mechanism involved in the sustained release of DOX from DOXM suspended in PLGA-PEG-PLGA is not clear. Temperature-sensitive polymeric gels such as PLGA-PEG-PLGA remain in solution form at room temperature and as gels at body temperature. At room temperature, the hydrogen

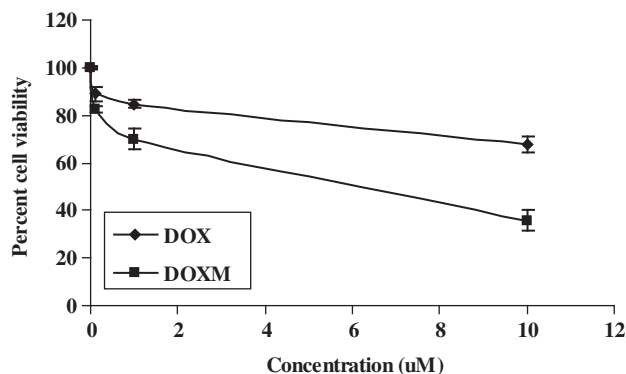


FIG. 7. Cell viability studies of DOX in Y-79 cells following treatment with DOX and DOXM.

bonding between the water molecules and PEG chains dominate and forces the copolymer molecules to stay in solution. At body temperature, the hydrophobic forces among the PLGA segments dominate and hydrogen bonding becomes weaker, thus leading to sol-gel transition. The release of drugs from the hydrogels mainly occurs by 2 mechanisms: (1) initial phase consists of drug diffusion from the hydrogel and (2) later phase consists of erosion hydrogel matrix.³⁹ The external surface of polymeric micelles is hydrophilic in nature and tends to partition in the PEG domains (Fig. 8). We anticipate that during the initial phase the polymeric micelles (~70–100 nm) tend to slowly diffuse through the hydrophilic porous channels, whereas in the later stage the release may be due to a combination of diffusion and erosion of the polymeric gel matrix. Moreover, it is likely that thermosensitive polymers upon gelation at body temperature (34°C–37°C) prevent the dilution of DOXM from the external fluids. Hence, these polymeric micelles may remain intact inside the thermosensitive gels and gradually release its cargo as the gel degrades. The release of DOXM from PLGA-PEG-PLGA gels acts as the major rate-limiting step in the release rate of DOX.

Qualitative uptake analysis with confocal imaging of Y-79 cells overexpressing folate receptor revealed that DOXM exhibits a much larger extent of cellular uptake than pure DOX. This was further confirmed by quantitative uptake studies. Z-stack images clearly depict the internalization of DOXM in Y-79 cells. DOX is a well-known substrate for MDR1 efflux pumps, which are highly expressed on Y-79 cells. These efflux pumps lower the entry of DOX into Y-79 cells.¹⁸ However, DOXM enter the cells via folate receptors on the surface of Y-79 cells. PEG acts as a linker between PLGA and folate moiety to form nanomicelles such that folate can easily bind to the folate receptor on Y-79 cells. With equivalent drug loading in the culture medium, DOXM showed much higher cell cytotoxicity than DOX in Y-79 cells. Huang *et al.* reported that the expression of folate receptor is much higher on the basolateral side of ARPE-19 cells when compared with the apical side.⁴⁰ This shows that DOX when administered as polymeric micelles conjugated to folic acid

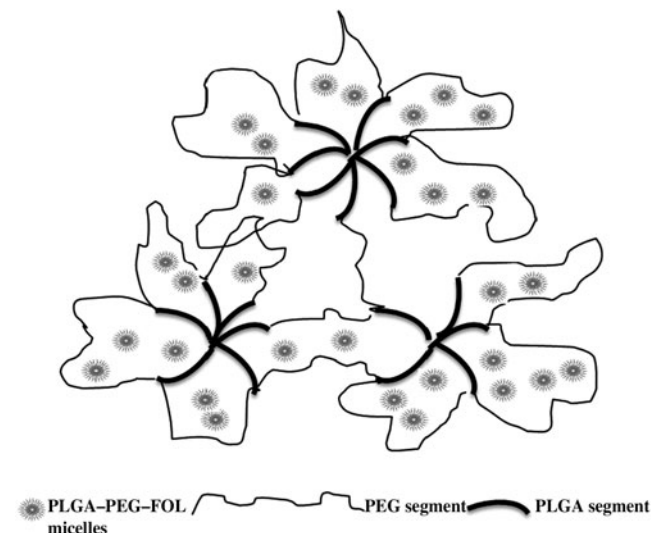


FIG. 8. Release mechanism of DOXM from PLGA-PEG-PLGA thermosensitive gel.

can specifically target the RB cells sparing the healthy retinal cells, which do not express folate receptor.

Previous studies from our laboratory concluded that IVT delivery of ganciclovir-loaded PLGA microspheres in PLGA-PEG-PLGA gel resulted in therapeutic vitreal concentrations for 14 days.³⁰ Moreover, this formulation did not produce any major breakdown in the retinal cell structure. We anticipate that our current formulation will be safe for the healthy retinal cells and toxic for the RB cells.

Conclusion

In summary, we have provided proof for a novel injectable drug carrier system for the local and targeted delivery of drugs to RB cells using DOX as a model drug. Release of DOX from DOXM was successfully retarded by PLGA-PEG-PLGA gel system. Qualitative uptake studies revealed that DOXM exhibited higher cellular uptake than pure DOX in Y-79 cells overexpressing folate receptors. This result was further confirmed from the quantitative uptake studies. Polymeric micellar systems suspended in thermosensitive gels may provide sustained and targeted delivery of anticancer agents (topotecan, etoposide, carboplatin, and vincristine) to RB cells.

Acknowledgments

The authors are thankful to Dr. Swapan K. Samanta for helping in the synthesis of PLGA-PEG-folate, Dr. Pal for helping in cell culture work, and Dr. Ferrari, School of Biological Sciences, for helping in confocal studies. This work was supported by the National Institutes of Health grants R01 EY 09171-16 and R01 EY 10659-12 and Missouri Life Sciences Research Grant No. MLRSB0017025.

Author Disclosure Statement

No competing financial interests exist.

References

- Albert, D.M. Historic review of retinoblastoma. *Ophthalmology* 94:654–662, 1987.
- Bishop, J.O., and Madson, E.C. Retinoblastoma. Review of the current status. *Surv. Ophthalmol.* 19:342–366, 1975.
- Honavar, S.G., and Singh, A.D. Management of advanced retinoblastoma. *Ophthalmol. Clin. North Am.* 18:65–73, 2005.
- Sanchez de Toledo, J. Retinoblastoma. Can we do more? *Clin. Transl. Oncol.* 10:525–526, 2008.
- Pesin, S.R., and Shields, J.A. Seven cases of trilateral retinoblastoma. *Am. J. Ophthalmol.* 107:121–126, 1989.
- Henkes, H.E., Henkes, H.E., and Oosterhuis, J.A. Tumors of the eye. *Doc. Ophthalmol.* 43:341–342, 1977.
- Aerts, I., Lumbroso-Le Rouic, L., Gauthier-Villars, M., Brisse, H., Doz, F., and Desjardins, L. Retinoblastoma. *Orphanet J. Rare Dis.* 1:31, 2006.
- De Potter, P. Current treatment of retinoblastoma. *Curr. Opin. Ophthalmol.* 13:331–336, 2002.
- Chintagumpala, M., Chevez-Barrios, P., Paysse, E.A., Plon, S.E., and Hurwitz, R. Retinoblastoma: review of current management. *Oncologist* 12:1237–1246, 2007.
- Eng, C., Li, F.P., Abramson, D.H., Ellsworth, R.M., Wong, F.L., Goldman, M.B., Seddon, J., Tarbell, N., and Boice, Jr., J.D. Mortality from second tumors among long-term survivors of retinoblastoma. *J. Natl. Cancer Inst.* 85:1121–1128, 1993.
- Beck, M.N., Balmer, A., Dessing, C., Pica, A., and Munier, F. First-line chemotherapy with local treatment can prevent external-beam irradiation and enucleation in low-stage intraocular retinoblastoma. *J. Clin. Oncol.* 18:2881–2887, 2000.
- Murphree, A.L., Villablanca, J.G., Deegan, W.F., 3rd, Sato, J.K., Malogolowkin, M., Fisher, A., Parker, R., Reed, E., and Gomer, C.J. Chemotherapy plus local treatment in the management of intraocular retinoblastoma. *Arch. Ophthalmol.* 114:1348–1356, 1996.
- Rizzuti, A.E., Dunkel, I.J., and Abramson, D.H. The adverse events of chemotherapy for retinoblastoma: what are they? Do we know? *Arch. Ophthalmol.* 126:862–865, 2008.
- Gallie, B.L., Budning, A., DeBoer, G., Thiessen, J.J., Koren, G., Verjee, Z., Ling, V., and Chan, H.S. Chemotherapy with focal therapy can cure intraocular retinoblastoma without radiotherapy. *Arch. Ophthalmol.* 114:1321–1328, 1996.
- Chin, K.V., and Liu, B. Regulation of the multidrug resistance (MDR1) gene expression. *In Vivo* 8:835–841, 1994.
- Kuo, M.T. Roles of multidrug resistance genes in breast cancer chemoresistance. *Adv. Exp. Med. Biol.* 608:23–30, 2007.
- Chan, H.S., Canton, M.D., and Gallie, B.L. Chemosensitivity and multidrug resistance to antineoplastic drugs in retinoblastoma cell lines. *Anticancer Res.* 9:469–474, 1989.
- Kartner, N., Evernden-Porelle, D., Bradley, G., and Ling, V. Detection of P-glycoprotein in multidrug-resistant cell lines by monoclonal antibodies. *Nature* 316:820–823, 1985.
- Li, B., Gao, R., Zhang, H., Li, L.Q., Gao, F., and Ren, R.J. [Studies on multidrug resistance associated protein in retinoblastoma]. *Zhonghua Yan Ke Za Zhi* 45:314–317, 2009.
- Janoria, K.G., Gunda, S., Boddu, S.H., and Mitra, A.K. Novel approaches to retinal drug delivery. *Expert Opin. Drug Deliv.* 4:371–388, 2007.
- Phylactos, A.C., and Unger, W.G. Biochemical changes induced by intravitreally-injected doxorubicin in the iris-ciliary body and lens of the rabbit eye. *Doc. Ophthalmol.* 95:145–155, 1998.
- Weitman, S.D., Lark, R.H., Coney, L.R., Fort, D.W., Frasca, V., Zurawski, Jr., V.R., and Kamen, B.A. Distribution of the folate receptor GP38 in normal and malignant cell lines and tissues. *Cancer Res.* 52:3396–3401, 1992.
- Shiokawa, T., Hattori, Y., Kawano, K., Ohguchi, Y., Kawakami, H., Toma, K., and Maitani, Y. Effect of polyethylene glycol linker chain length of folate-linked microemulsions loading aclacinomycin A on targeting ability and antitumor effect *in vitro* and *in vivo*. *Clin. Cancer Res.* 11:2018–2025, 2005.
- Yoo, H.S., and Park, T.G. Folate receptor targeted biodegradable polymeric doxorubicin micelles. *J. Control. Release* 96:273–283, 2004.
- Zhao, H., and Yung, L.Y. Selectivity of folate conjugated polymer micelles against different tumor cells. *Int. J. Pharm.* 349:256–268, 2008.
- Park, E.K., Kim, S.Y., Lee, S.B., and Lee, Y.M. Folate-conjugated methoxy poly(ethylene glycol)/poly(epsilon-caprolactone) amphiphilic block copolymeric micelles for tumor-targeted drug delivery. *J. Control. Release* 109:158–168, 2005.
- Yoo, H.S., and Park, T.G. Biodegradable polymeric micelles composed of doxorubicin conjugated PLGA-PEG block copolymer. *J. Control. Release* 70:63–70, 2001.
- Kansara, V., Paturi, D., Luo, S., Gaudana, R., and Mitra, A.K. Folic acid transport via high affinity carrier-mediated system in human retinoblastoma cells. *Int. J. Pharm.* 355:210–219, 2008.
- Duvvuri, S., Janoria, K.G., and Mitra, A.K. Development of a novel formulation containing poly(D,L-lactide-co-glycolide) microspheres dispersed in PLGA-PEG-PLGA gel

- for sustained delivery of ganciclovir. *J. Control. Release* 108: 282–293, 2005.
30. Duvvuri, S., Janoria, K.G., Pal, D., and Mitra, A.K. Controlled delivery of ganciclovir to the retina with drug-loaded poly(D,L-lactide-co-glycolide) (PLGA) microspheres dispersed in PLGA-PEG-PLGA gel: a novel intravitreal delivery system for the treatment of cytomegalovirus retinitis. *J. Ocul. Pharmacol. Ther.* 23:264–274, 2007.
 31. Aukunuru, J.V., Sunkara, G., Bandi, N., Thoreson, W.B., and Kompella, U.B. Expression of multidrug resistance-associated protein (MRP) in human retinal pigment epithelial cells and its interaction with BAPSG, a novel aldose reductase inhibitor. *Pharm. Res.* 18:565–572, 2001.
 32. Treupel, L., Poupon, M.F., Couvreur, P., and Puisieux, F. [Vectorisation of doxorubicin in nanospheres and reversion of pleiotropic resistance of tumor cells]. *C. R. Acad. Sci. III* 313:171–174, 1991.
 33. Gaudana, R., Jwala, J., Boddu, S.H., and Mitra, A.K. Recent perspectives in ocular drug delivery. *Pharm. Res.* 26:1197–1216, 2009.
 34. Jones, M., and Leroux, J. Polymeric micelles—a new generation of colloidal drug carriers. *Eur. J. Pharm. Biopharm.* 48:101–111, 1999.
 35. Bae, Y.H., and Yin, H. Stability issues of polymeric micelles. *J. Control. Release* 131:2–4, 2008.
 36. Chen, H., Kim, S., He, W., Wang, H., Low, P.S., Park, K., and Cheng, J.X. Fast release of lipophilic agents from circulating PEG-PDLLA micelles revealed by *in vivo* forster resonance energy transfer imaging. *Langmuir* 24:5213–5217, 2008.
 37. Jeon, H.J., Jeong, Y.I., Jang, M.K., Park, Y.H., and Nah, J.W. Effect of solvent on the preparation of surfactant-free poly(DL-lactide-co-glycolide) nanoparticles and norfloxacin release characteristics. *Int. J. Pharm.* 207:99–108, 2000.
 38. Liu, S.Q., Tong, Y.W., and Yang, Y.Y. Incorporation and *in vitro* release of doxorubicin in thermally sensitive micelles made from poly(N-isopropylacrylamide-co-N,N-dimethylacrylamide)-*b*-poly(D,L-lactide-co-glycolide) with varying compositions. *Biomaterials* 26:5064–5074, 2005.
 39. Qiao, M., Chen, D., Ma, X., and Liu, Y. Injectable biodegradable temperature-responsive PLGA-PEG-PLGA copolymers: synthesis and effect of copolymer composition on the drug release from the copolymer-based hydrogels. *Int. J. Pharm.* 294:103–112, 2005.
 40. Huang, W., Prasad, P.D., Kekuda, R., Leibach, F.H., and Ganapathy, V. Characterization of N5-methyltetrahydrofolate uptake in cultured human retinal pigment epithelial cells. *Invest. Ophthalmol. Vis. Sci.* 38:1578–1587, 1997.

Received: March 25, 2010

Accepted: June 11, 2010

Address correspondence to:

Dr. Ashim K. Mitra

Division of Pharmaceutical Sciences

School of Pharmacy

University of Missouri-Kansas City

2464 Charlotte Street

Kansas City, MO 64108-2718

E-mail: mitraa@umkc.edu